

# Characterization techniques for thin and thick ferroelectric films

A. Deleniv\*

*Department of Microtechnology and Nanoscience, Chalmers University of Technology, Sweden*

Available online 15 December 2006

## Abstract

A few measurement techniques are presented for characterization of thin and thick ferroelectric films at microwave frequencies. Broadband reflection type measurements using a probe station are considered for on wafer characterization of thin films. The accuracy of the method is analyzed with respect to measurement residual systematic errors. A test structure is introduced allowing quick and accurate extraction of the film parameters based on the rigorous full-wave model. Two measurement techniques are reported for electrode-less characterization of thick ferroelectric films. The first method (X-band) is based on the reflection type measurement of a resonator established by a layered alumina/ferroelectric sample loaded in a cut-off waveguide. The second method (B-band) utilizes an open resonator (OR) technique. Theoretical and experimental results are presented. © 2006 Elsevier Ltd. All rights reserved.

**Keywords:** Films; Ferroelectrics; Dielectric properties; Impedance

## 1. Introduction

Even though ferroelectric films have been the subject of intensive study during the last three decades, there still are issues to be solved concerning their accurate characterization at microwave frequencies. An accurate characterization technique was recently elaborated using split post dielectric resonator.<sup>1</sup> However, this approach requires a separate test sample and, therefore, cannot be used to characterize thin film locally. Additionally, split post resonator does not support characterization of thin ferroelectric films deposited on top of an electrode, which is often required in practice. Therefore, one often prefers less accurate characterization technique, which use a probe station to measure an impedance of especially designed test structures (varactors) in broad frequency range. The reliability of such an approach is often questionable<sup>2</sup> because of the measurement uncertainties and accuracy of the test structure modeling. The first section of this paper addresses both these issues. A measurement routine is proposed that substantially improves the measurement accuracy. A test structure is introduced allowing the use of a multilayered substrate. This is equipped with a rigorous, although a simple full-wave model. It is shown that the impedance method using the above test structure is an accurate and reliable tool to characterize ferroelectric thin films.

Following this, two resonance techniques for electrode-less characterization of thick ferroelectric films are then discussed. The partially filled waveguide technique<sup>3</sup> is utilized for measurement of thick films in X-band, while the open resonator technique<sup>4</sup> is employed in B-band. The above resonance measurements are important to distinguish intrinsic losses of ferroelectric films, which is difficult or even impossible with techniques utilizing electrodes. This is mainly due to interfacial layers with high losses that often accompany interfaces with electrodes.

## 2. Thin film characterization using impedance measurements

Broadband reflection type measurements are widely used today to characterize thin ferroelectric films (dielectric permittivity and losses), which are comprised of two essentially different stages. The first stage involves a probe station for measuring the impedance of especially designed test structure (hereafter DUT) and is associated with the measurement uncertainties. These are translated through the retrieval procedure (this comprises the second stage of the film characterization) into uncertainties of the film parameters and, therefore, should be carefully examined.

In general, any DUT (capacitor/varactor) use a layered substrate stack (thin ferroelectric film may be one of many layers) with metal electrodes on the top of it. Irrespective of the specific substrate structure and design of the electrodes, the

\* Tel.: +46 31 7723605; fax: +46 31 164513.

E-mail address: [anatoli.deleniv@mc2.chalmers.se](mailto:anatoli.deleniv@mc2.chalmers.se).

total capacitance,  $C_{\text{DUT}}$ , and the loss tangent,  $\tan \delta_{\text{DUT}}$ , of any DUT can be defined as below:

$$C_{\text{DUT}} = \sum_{i=1}^N C_i, \quad (1)$$

$$\tan \delta_{\text{DUT}} = \frac{1}{Q_{\text{electr.}}} + \sum_{i=1}^N (k_i \tan \delta_i), \quad (2)$$

$$k_i = \frac{C_i}{C_{\text{DUT}}}. \quad (3)$$

$C_i$  and  $k_i$  are defined for each layer,  $i = 1, 2, \dots, N$ , corresponding, respectively, to the partial capacitance and the inclusion rate, while  $Q_{\text{electr.}}$  is the  $Q$ -factor of the electrodes. The purpose of the measurements is to accurately characterize the complex permittivity  $\varepsilon_m$  of the  $m$ th layer, which is the only one with unknown parameters. Assuming that the retrieval procedure provides an absolute accuracy (this will be discussed in more detail later), the following two identities define the final errors for the parameters of the  $m$ th layer:

$$\frac{\Delta \varepsilon_m}{\varepsilon_m} \equiv \frac{\Delta C_m}{C_m} = \frac{1}{k_m} \frac{\Delta C_{\text{DUT}}}{C_{\text{DUT}}} \quad (4)$$

$$\frac{\Delta \tan \delta_m}{\tan \delta_m} = \left( 1 - \frac{1}{\tan \delta_{\text{DUT}}} \left( \frac{1}{Q_{\text{electr.}}} - \sum_{i=1; i \neq m}^N k_i \tan \delta_i \right) \right)^{-1} \times \frac{\Delta \tan \delta_{\text{DUT}}}{\tan \delta_{\text{DUT}}} \quad (5)$$

(4) and (5) indicate that even small measurement errors can be “amplified” by an improper design of the DUT—the size of the electrodes and choice of the layers directly affect the inclusion rate  $k_i$  of each layer. As a first step we discuss the impact of the measurement uncertainty on the capacitance and  $Q$ -factor of the DUT. When using a VNA we are subjected to the residual systematic errors established during the calibration process. Effective directivity and source match—these are the two most important error contributors when dealing with one-port DUT. Considering the high quality of the modern VNAs, the values of the above residuals are mostly due to calibration type and accuracy of the utilized standards. The joint effect of the above errors is represented by an equivalent parasitic vector,  $\Delta \tilde{S} = \rho_{\text{unc}} e^{j\phi}$ , interfering with the useful signal. The effect of the measurement uncertainties on the measured capacitance and  $Q$ -factor is thoroughly analyzed<sup>5</sup> for reactors with high- $Q$  ( $Q_{\text{DUT}} > 50$ ). The following formulas for the errors were obtained:

$$\left| \frac{\Delta \bar{B}}{\bar{B}_{\text{DUT}}} \right| = |\Delta \tan \delta_{\text{DUT}}|$$

$$= \left| \rho_{\text{unc}} \cos(\xi) \left[ 1 + \left( \frac{1 - \bar{B}_{\text{DUT}}^2}{2\bar{B}_{\text{DUT}}} \right)^2 \right] \right|, \quad (6)$$

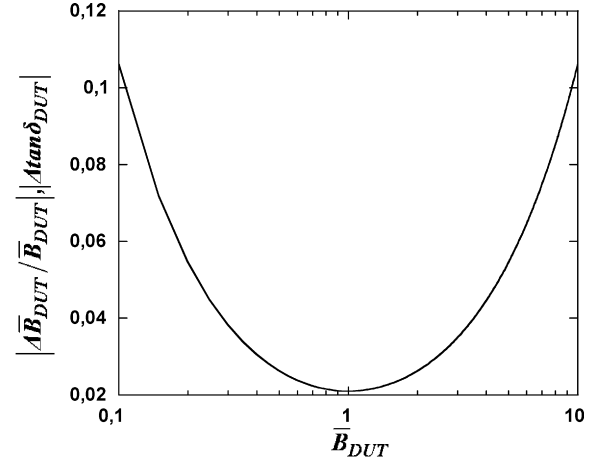


Fig. 1. Measurement uncertainties for a high- $Q$  DUT.

$$\xi = a \tan \left( \frac{1 - \bar{B}_{\text{DUT}}^2}{2\bar{B}_{\text{DUT}}} \right). \quad (7)$$

Here,  $\bar{B}_{\text{DUT}} = \omega C_{\text{DUT}} 50$  is a normalized admittance of the DUT. The expressions (6) and (7) were used to obtain the uncertainty curves shown in Fig. 1. The effective directivity  $-42$  dB and source match  $-38$  dB were used here to define  $\rho_{\text{unc}}$ . These data are defined for the full two-port calibration with sliding loads using 85056A 2.4 mm calibration kit.<sup>6</sup> It is noted that the smallest errors are expected for  $\bar{B}_{\text{DUT}} = 1$ . While the capacitance  $C_{\text{DUT}}$  can be measured with  $\sim 2\%$  accuracy, an unacceptable error is obtained for the effective loss tangent. The obtained results agree well with those recently reported<sup>2</sup> and seem discouraging, since even high precision on-wafer calibration standards do not provide better calibration accuracy<sup>7</sup>—the effective directivity and the source match are compatible with those mentioned above.

At this point it is important to be reminiscent that we deal with systematic residuals errors—these are unique and perfectly repeatable for any separately taken DUT (measurement repeatability using 67A probe model from “Picoprobe” is  $-80$  dB). Therefore, the uncertainty can be efficiently eliminated if an additional standard is available with the reactance identical to that of DUT and high  $Q$ -factor. It can be shown that the error of the measurement in that case is reduced by a factor  $\sim Q_{\text{DUT}}$ —this is far better accuracy prediction as compared to that in Fig. 1. The required standards are easily realized using high- $Q$  MgO, Si or  $\text{LaAl}_2\text{O}_3$  substrates. Typically, one should prefer  $\text{LaAl}_2\text{O}_3$  having the highest dielectric permittivity,  $\varepsilon_r \approx 23.7$ —the test structures using thin ferroelectric films may have rather high capacitances. The proposed procedure is then summarized as below:

- (1) DUT is measured ( $\tilde{S}_{11}^{\text{DUT}}$ ) and  $C_{\text{DUT}}$  is defined at the frequency of the best accuracy ( $\bar{B}_{\text{DUT}} = 1$ );
- (2) an additional standard having  $C_{\text{STD}} = C_{\text{DUT}}$  and  $Q_{\text{STD}} \gg Q_{\text{DUT}}$  is measured so that the equivalent parasitic vector,  $\Delta \tilde{S}$ , can be defined;

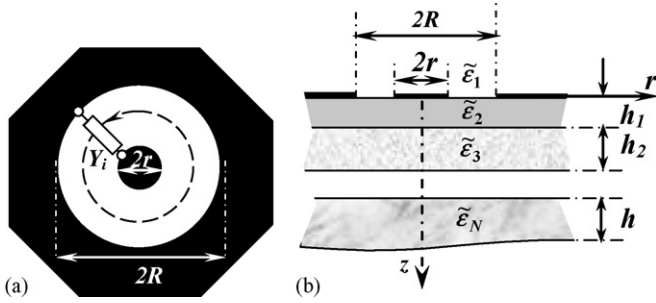


Fig. 2. Layout (a) and cross-section (b) of the test-structure.

- (3) the film parameters are then retrieved using  $\tilde{S}_{11} = \tilde{S}_{11}^{\text{DUT}} - \Delta\tilde{S}$ .

The retrieval routine typically employs a root searching algorithm in conjunction with a model of the test structure. It is clear that the accuracy of the model is defining that of the retrieval routine. Conformal mapping is a popular technique often used to build such models providing useful analytic approximations. However, use of rigorous numerical techniques provides much better accuracy. Whereas commercial software usually provides great flexibility, there are few situations making their use quite difficult or even impossible. This is the case when considering an electrically thin layer with high dielectric permittivity, which is adjacent to the electrodes. The problem is resolved with the model addressing specifics of the mentioned above structures.<sup>8</sup> The layout and the cross-section of the proposed test structure are shown in Fig. 2a and b, respectively. This comprises circularly shaped electrodes on the top of the multilayered substrate characterized by  $\tilde{\epsilon}_i$  and  $h_i$ ,  $i = 1, 2, \dots, N$ .

The model is based on the stationary formula for admittance solved in the Hankel transform domain (HTD) via Galerkin's technique. The electrically small size of the test structure and its symmetry greatly simplifies modeling—it is reduced to tackling a few path integrals using a set of predefined expansion functions with correct edge behaviour. The latter is chosen specifically so that in combination with known asymptotic forms of the Green's function, all scalar products can be obtained analytically. Therefore, any kind of numerical problems is avoided.

The cross-section of a test structure substrate and the measured capacitance,  $C_{\text{DUT}}$ , are shown in Fig. 3. The test structure is used here to measure the properties of thin STO layer—the only layer with unknown parameters. Three different electrode options were used in the measurements with a fixed outer radius,  $R = 100 \mu\text{m}$ . The capacitances were simulated for these test structures assuming  $\epsilon_r^{\text{STO}} = 115$ . Simulated data are marked by small crosses (Fig. 3) at  $\sim 22.5 \text{ GHz}$ —this is the frequency optimal for the measurement of the test structure with  $7.5 \mu\text{m}$  aperture. While perfect agreement is observed for  $7.5 \mu\text{m}$  and  $22.5 \mu\text{m}$  wide apertures, nearly 8% mismatch is indicated for the one with  $5 \mu\text{m}$ . A possible reason can be a slight deviation in the aperture size—using  $4.5 \mu\text{m}$  instead provides perfect match of simulation and the experiment.

At frequencies above 3 GHz, the contribution of the STO layer is dominating the total DUT loss.<sup>8</sup> Therefore, the loss of the STO layer, can be directly related to that of DUT using the

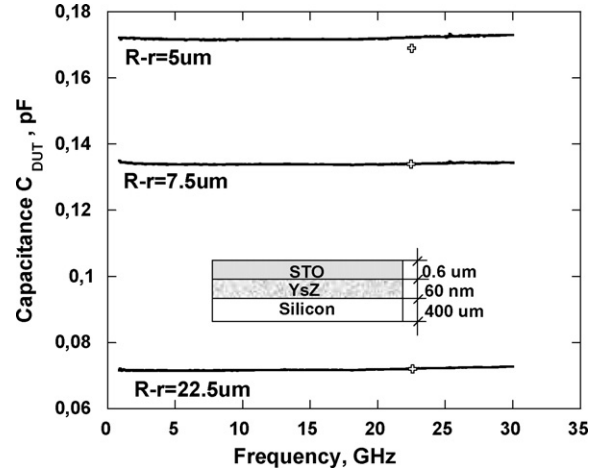


Fig. 3. Measured capacitance for the structure with corresponding cross-sectional view.

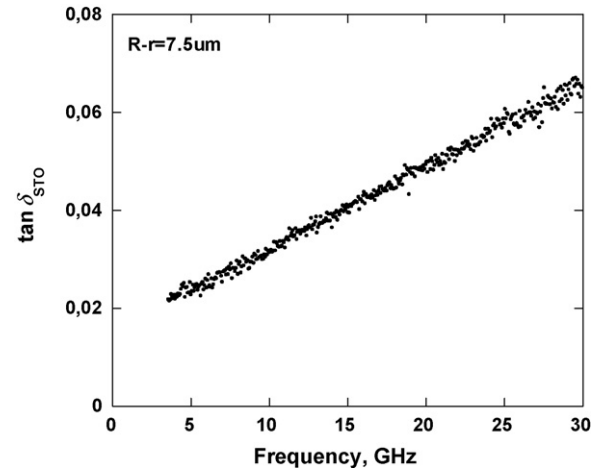


Fig. 4. Measured  $\tan \delta_{\text{STO}}$  of the STO layer.

layer inclusion rate,  $k_{\text{STO}}$ :

$$\tan \delta_{\text{STO}} \approx \frac{\tan \delta_{\text{DUT}}}{k_{\text{STO}}} \quad (8)$$

The latter is found<sup>8</sup> to be  $k_{\text{STO}} = 0.37$  for the test structure with the aperture size  $7.5 \mu\text{m}$ . The measurement data are corrected using a measurement of an additional standard, which is then used to define  $\tan \delta_{\text{STO}}$  (Fig. 4). It is interesting to note that the measurement is in good agreement with the predicted linear behaviour.<sup>9</sup>

### 3. X-band characterization of thick films using a partially filled waveguide

The longitudinal section of the measurement set-up is shown in Fig. 5. It consists of two bolted parts—standard WG to SMA adapter and resonator. The resonator is comprised of a section of cut-off WG loaded by a two-layered sample. The cross-sectional dimensions of the WG are chosen so that no higher order modes propagate in the frequency band of the used adapter. The unloaded section of the cut off WG is open ended with sufficient

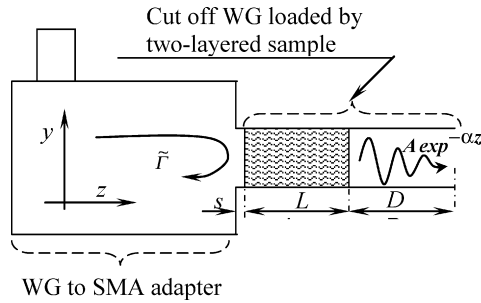


Fig. 5. A longitudinal section of the measurement set-up.

length of empty section to ensure that no radiation occurs. The photo of the WG assembly and cross-section of the sample are shown in Fig. 6 and inset, respectively. The two-layered slab is clamped between two teflon holders to ensure a correct and controllable distance  $l$  from the sample to the sidewalls of the WG. In Fig. 6,  $h_A$  denotes the thickness of the alumina substrate and  $h_F$  is the thickness of the film. Assuming that there are no gaps between the sample and WG such configuration supports TM-to-x and TE-to-x modes making the problem perfectly suited for transverse resonance method (TRM).

There are two main error sources to be dealt with considering the application of this method. The first error source is due to the uncertainty of the size of the air gap, which unavoidably exists between the sample and WG walls. This uncertainty is tracked through the entire retrieval procedure leading to uncertainty in the finally obtained film parameters. Taking the presence of an air-gap as a fact, one may try to reduce its effect by filling it with a properly chosen dielectric. We propose to use vaseline, which has dielectric properties quite similar to teflon ( $\epsilon_r^{\text{Vas.}} = 2.16$ ;  $\tan \delta \approx 0.01$  at 10 GHz). It is verified<sup>3</sup> that by doing so the accuracy of the measurements is improved by a factor of two. The second source of errors is due to reactance's appearing between the empty and filled sections of the cut off WG. Strictly speaking, this is not a problem if a rigorous software tool (HFSS, Microwave Studio, etc.) is used to analyze the resonator. However, using computationally complex techniques

Table 1

Details of measurements and retrieved film parameters

$f_{\text{res}}$ (GHz)	$Q$	$10^3 \tan \delta$		$\epsilon_r$	
		$\Delta l = 0$ mm	$\Delta l = 1.65$ mm	$\Delta l = 0$ mm	$\Delta l = 1.65$ mm
8.875	81	$\sim 31 \pm 1$	$\sim 39 \pm 1$	$270 \pm 17$	$231 \pm 15$
10.160	77	$\sim 30 \pm 1$	$\sim 40 \pm 1$	$283 \pm 17$	$231 \pm 15$
11.590	72	$\sim 31 \pm 1$	$\sim 42 \pm 1$	$281 \pm 17$	$225 \pm 15$
8.705	79	$\sim 31 \pm 1$	$\sim 40 \pm 1$	$298 \pm 18$	$231 \pm 15$
10.480	72	$\sim 29 \pm 1$	$\sim 41 \pm 1$	$333 \pm 20$	$240 \pm 15$

makes the retrieving procedure more cumbersome and time consuming. The problem is avoided by measuring two samples with different lengths. Then, the length of each ideally terminated sample is assumed to be:

$$L_{1(2)}^{\text{ass.}} = L_{1(2)} + 2 \Delta l, \quad (9)$$

where  $\Delta l$  is the sample extension due to junction reactance. The latter is used as a variable when retrieving the complex dielectric constant of the thick film with TRM. The value of  $\Delta l$  is optimized until good agreement in the film parameters obtained for the above two samples is achieved.

The data of two measurements using 30 mm and 20 mm long samples are collected in Table 1. The thickness of the alumina substrate is 1.02 mm ( $\epsilon_r = 9.16$ ), while the thick film thickness is  $30 \pm 2 \mu\text{m}$ . The first three rows of Table 1 contain data for a 30 mm long sample—the others are reserved for a 20 mm long one. According to Table 1, an accuracy within 5% is observed for thick film parameters for all experimentally obtained resonances using  $\Delta l = 1.65$  mm. The residual uncertainty of the film parameters is due to a  $\pm 2 \mu\text{m}$  deviation in the film thickness and uncertainty of the size of the vaseline-filled gap.

The introduced resonator can be scaled to make measurements at other frequencies. However, at higher frequencies the test sample becomes impractically small and difficult to handle. In such cases an open resonator technique provides a solution to the thick film characterization problem.

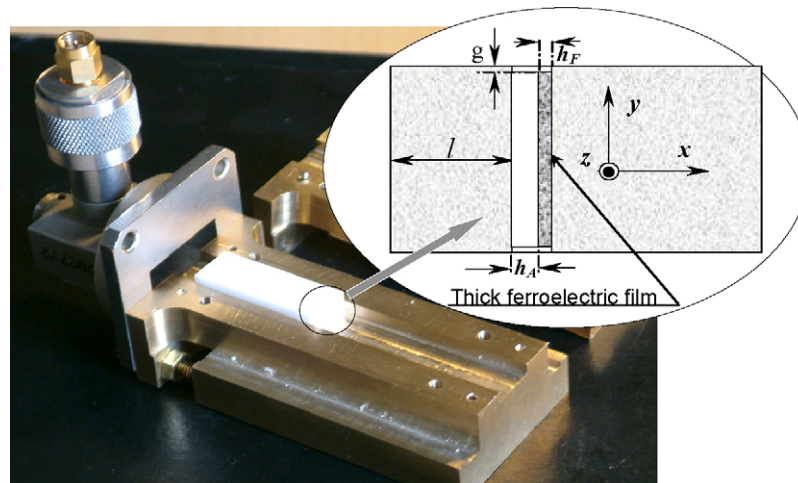


Fig. 6. A measurement assembly with the upper half of the cut-off WG removed.



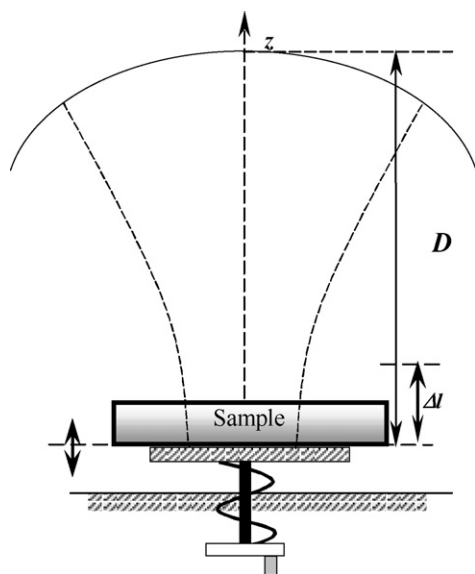


Fig. 7. An open resonator apparatus.

#### 4. B-band characterization of thick films using open resonator

The application of open resonators (OR) for characterization of dielectrics at microwave is a well established technique and has a number of advantages over closed cavities:

- OR is more accessible than closed cavities and does not require dismounting for sample insertion;
- the mode spectrum of OR is sparser, this reduces the likelihood of errors due to mode coincidences;
- their  $Q$ -factors are higher than cavities of similar volume;
- only the cross-section of the dielectric specimen is critical, provided its radius is greater than that of the beam.

Until recently the OR technique was mostly restricted to measurements of one-layer dielectrics with relatively low dielectric constants. The first experimental results on the measurement of ferroelectric films are reported in<sup>10</sup>. There, the authors used a transverse resonance technique with a TEM approximation of the field in the layered sample. More rigorous vector field theory of the open resonator<sup>11</sup> is extended to cover multilayered dielectric plates<sup>4</sup> and verified via measurement of thick ferroelectric films. The latter is usually fabricated on dielectric (alumina or MgO) plates and can be directly used as a test structure provided that their size is sufficient to intercept the beam.

An open resonator is schematically shown in Fig. 7. The measurement procedure comprises of two steps. First,

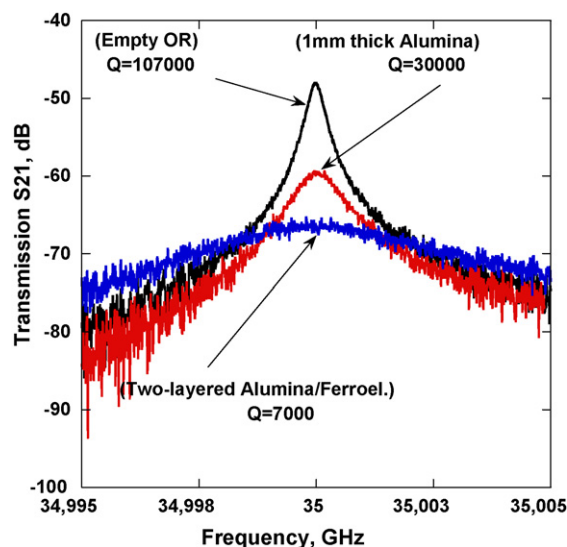


Fig. 8. Typical resonance curves using OR.

the empty resonator is characterized at a fixed frequency, which in theory is an arbitrary frequency in the WG adapter band. This step is used to set the length  $D$  of the resonator and measure its quality factor  $Q$  for the utilized  $TEM_{0,0,q}$  mode (the typical value is  $Q > 10^5$ ). Next, the sample is loaded in the OR thereby shifting the resonance down in frequency (the resonator becomes electrically longer). The lower plate mirror of the OR is moved up ( $\Delta l$ /mm), until the resonance is re-established at the measurement frequency. The quality factors  $Q$  and  $Q_1$  and the lengths  $D$  and  $D - \Delta l$  of the empty and loaded resonators, respectively, provide all necessary input for the processing stage of the characterization procedure.

Typical resonance curves for the empty OR and the one loaded with two different samples are shown in Fig. 8 along with their measured  $Q$ -factors. It is noted that for a two-layered alumina/ferroelectric sample the measurement may be quite noisy as it approaches the noise floor of the instrument. To reduce this noise one typically should get the greatest dynamic range of the VNA. This can be achieved using as high as possible source output (this is limited by the maximum input of the receiver) and also high averaging factors.

Table 2 contains the measurement data and the retrieved parameters for the three different  $Al_2O_3$ /BSTO two-layered samples ( $5\text{ cm} \times 5\text{ cm}$ ) at 35 GHz and 39 GHz, respectively. Sample A1 from Table 2 is also measured using the above-discussed WG technique in X-band. Comparison of data presented in both tables provides good evidence of their reliability as the methods produce self-consistent data.

Table 2  
Details of measurements on alumina/ferroelectric samples at 35 GHz and 39 GHz

Thickness of $Al_2O_3$ /BSTO layers ( $\mu\text{m}$ )	$\Delta l$ ( $\mu\text{m}$ )/ $Q_1$ , 35 GHz	Extracted $\epsilon_r/\tan \delta$	$\Delta l$ ( $\mu\text{m}$ )/ $Q_1$ , 39 GHz	Extracted $\epsilon_r/\tan \delta$
Sample A1 1020/22	3091/4000	$194 \pm 25/0.130 \pm 0.004$	2716/5600	$203 \pm 33/0.176 \pm 0.007$
Sample A2 1019/30	3129/3880	$201 \pm 22/0.142 \pm 0.004$	2736/5150	$212 \pm 31/0.192 \pm 0.007$
Sample A3 1010/43	3163/4800	$189 \pm 17/0.126 \pm 0.004$	2747/6300	$181 \pm 23/0.157 \pm 0.005$

## 5. Conclusion

Three different techniques for the characterization of thin and thick ferroelectric films at microwave frequencies are introduced in this paper. All methods are verified via practical examples demonstrating their practical value and accuracy.

## References

1. Krupka, J., Huang, W.-T. and Tung, M.-J., Complex permittivity measurements of thin ferroelectric films employing split post dielectric resonator. In *Proceedings of IMF11*, 2005 [Presentation No. 06-021].
2. Petrov, P. K., McN Alford, N. and Gevorgian, S., Techniques for microwave measurements of ferroelectric thin films and their associated error and limitations. *Meas. Sci. Technol.*, 2005, **16**, 583–589.
3. Deleniv, A., Gevorgian, S., Jantunnen, H. and Hu, T., Microwave characterization of ferroelectric ceramic films. In *Proceedings of EuMC*, 2004, pp. 541–544.
4. Deleniv, A. and Gevorgian, S., Open resonator technique for measuring multilayered dielectric plates. *IEEE Trans. Microw. Theory Tech.*, 2005, **53**, 2908–2916.
5. Deleniv, A. and Gevorgian, S., Characterization accuracy of high- $Q$  reactors using broadband reflection/transmission measurement techniques. In *Proceedings of EuMC*, 2006, Manchester, UK, pp. 975–978.
6. Agilent 8510C Network Analyzer Data Sheet, Agilent Technologies.
7. Oldfield, B., Wafer probe calibration accuracy measurements. In *Proceedings of the 48th ARFTG Conf. Dig.*, 1996.
8. Deleniv, A., Abadei, S. and Gevorgian, S., Microwave characterization of thin ferroelectric films. In *Proceedings of EuMC*, 2003, pp. 483–486.
9. Tagantsev, A. K., Sherman, V. O., Astafiev, K. F., Venkatesh, J. and Setter, N., Ferroelectric materials for microwave tuneable applications. *J. Electroceram.*, 2003, **11**, 5–66.
10. Buslov, O. Y., Keys, V. N., Kozyrev, A. B., Kotelnikov, I. V. and Kulik, P. V., Procedure of measurement of ferroelectric films parameters using open resonator method. In *Proceedings of CriMiCo*, 2003, p. 684 [IEEE Catalog Number: 03EX697].
11. You, P. K. and Cullen, A. L., Measurement of permittivity by means of an open resonator. I. Theoretical. *Proc. Roy. Soc. Lond. A*, 1982, **380**, 49–71.